OPEN ACCESS

ORIGINAL RESEARCH

FLCN-regulated miRNAs suppressed reparative response in cells and pulmonary lesions of Birt-Hogg-Dubé syndrome

Haiyan Min,[1,2] Dehua Ma,[3] Wei Zou,[4] Yongzheng Wu,[1,2] Yibing Ding,[1,2] Chengchu Zhu,[3] Anqi Lin,[1,2] Shiyu Song,[1,2] Qiao Liang,[1,2] Baofu Chen,[3] Bin Zhang,[1] Yueming Wan,[5] Minhua Ye,[3] Yanqing Pan,[4] Yanting Wen,[1,2] long Yi,[1,2] Qian Gao [1,2]

► Additional material is published online only. To view please visit the journal online (http://dx.doi.org/10.1136/thoraxjnl-2019-213225).

For numbered affiliations see end of article.

Correspondence to
Professor Qian Gao, Jiangsu Key Laboratory for Molecular Medicine, Nanjing University Medical School, Nanjing 210093, China;
qian_gao@nju.edu.cn

HM and DM contributed equally.

Received 13 February 2019
Revised 21 December 2019
Accepted 28 January 2020
Published Online First 17 March 2020

ABSTRACT

Background Birt-Hogg-Dubé Syndrome (BHDS) characterised by skin fibrofolliculomas, kidney tumour and pulmonary cysts/pneumothorax is caused by folliculin (FLCN) germline mutations. The pathology of both neoplasia and focused tissue loss of BHDS strongly features tissue-specific behaviour of the gene. Isolated cysts/pneumothorax is the most frequent atypical presentation of BHDS and often misdiagnosed as primary spontaneous pneumothorax (PSP). Deferential diagnosis of BHDS with isolated pulmonary presentation (PSP-BHD) from PSP is essential in lifelong surveillance for developing renal cell carcinoma.

Methods The expression profiles of microRNAs (miRNAs) in cystic lesions of PSP-BHD and PSP were determined via microarray. The selected upregulated miRNAs were further confirmed in the plasma of an expanded cohort of PSP-BHD patients by reverse transcription quantitative PCR (RT-qPCR). Their diagnostic accuracy was evaluated. Moreover, the cellular functions and targeted signalling pathways of FLCN-regulated miRNAs were assessed in various cell lines and in the lesion tissue contexts.

Results Cystic lesions of PSP-BHD and PSP showed different miRNAs profiles with a significant upregulation of miR-424–5p and let-7d-5p in PSP-BHD. The combination of the two effectively predicted BHDS patients. In vitro studies revealed a suppressive effect of FLCN on miR-424–5p and let-7d-5p expressions specifically in lung epithelial cells. The ectopic miRNAs triggered epithelial apoptosis and epithelial transition of mesenchymal cells and suppressed the reparative responses in cells and tissues with FLCN deficiency.

Conclusion The upregulation of miR-424–5p and let-7d-5p by FLCN deficiency occurred in epithelial cells and marked the PSP-BHD condition, which contributed to a focused degenerative pathology in the lung of PSP-BHD patients.

Key messages

What is the key question?

► Varied pathological presentations of Birt-Hogg-Dubé syndrome (BHDS) indicate tissue-specific function of the causal gene folliculin (FLCN), which was widely studied mechanistically in the kidney tumours but poorly elucidated in lung cysts/pneumothorax presentation.

What is the bottom line?

► FLCN negatively regulated miR-424–5p and let-7d-5p expressions specifically in lung epithelial cells, and thus caused a significant increase of the two in both lung tissue and circulation in FLCN mutant BHD patients, which resulted in an increased apoptosis of lung epithelial cells and mesenchymal–epithelial transition of fibroblasts, qualified them as diagnostic markers for disease screen.

Why read on?

► The mechanism revealed in this study is specific to the lung, and implies that the miRNAs regulated by FLCN suppressed cell reparative response in the lung tissue and contributed to a focused degenerative pathology in BHDS' lung.

Linked

► http://dx.doi.org/10.1136/thoraxjnl-2019-214112
► http://dx.doi.org/10.1136/thoraxjnl-2020-214861

Check for updates

To cite: Min H, Ma D, Zou W, *et al*. *Thorax* 2020;**75**:476–485.

INTRODUCTION

Birt-Hogg-Dubé syndrome (BHDS) characterised by skin fibrofolliculomas, pulmonary cysts/pneumothorax and increased risk of kidney cancers is an autosomal dominant disease caused by germline mutations of folliculin (FLCN) gene.[1] It is often misdiagnosed as primary spontaneous pneumothorax (PSP) in particular in the cases with only isolated lung cysts/pneumothorax presentation (PSP-BHD).[2–4] An early and definitive recognition of PSP-BHD that is broadly underdiagnosed from PSP is necessary for a lifelong surveillance due to an increased risk for developing kidney tumours.[5–7]

Genetic analysis of FLCN gene consists of sequence analysis and exonic deletion and amplification detection.[8] With this approach, we have previously found in a cohort study that about 10% of hospitalised PSP patients who were not considered to initiate a genetic examination of FLCN gene were actually BHDS suffers.[2] Thus, a screen of PSP population with a technically simpler and more affordable tool before a genetic analysis of BHDS is desirable.

microRNAs (miRNAs) have been served as the signature for various diseases including genetic disorders.[9–11] In fact, a robust miRNA signature often indicates a mechanistic role of the targets of miRNAs in the disease development, and thus composes of an effective tool to dissect disease

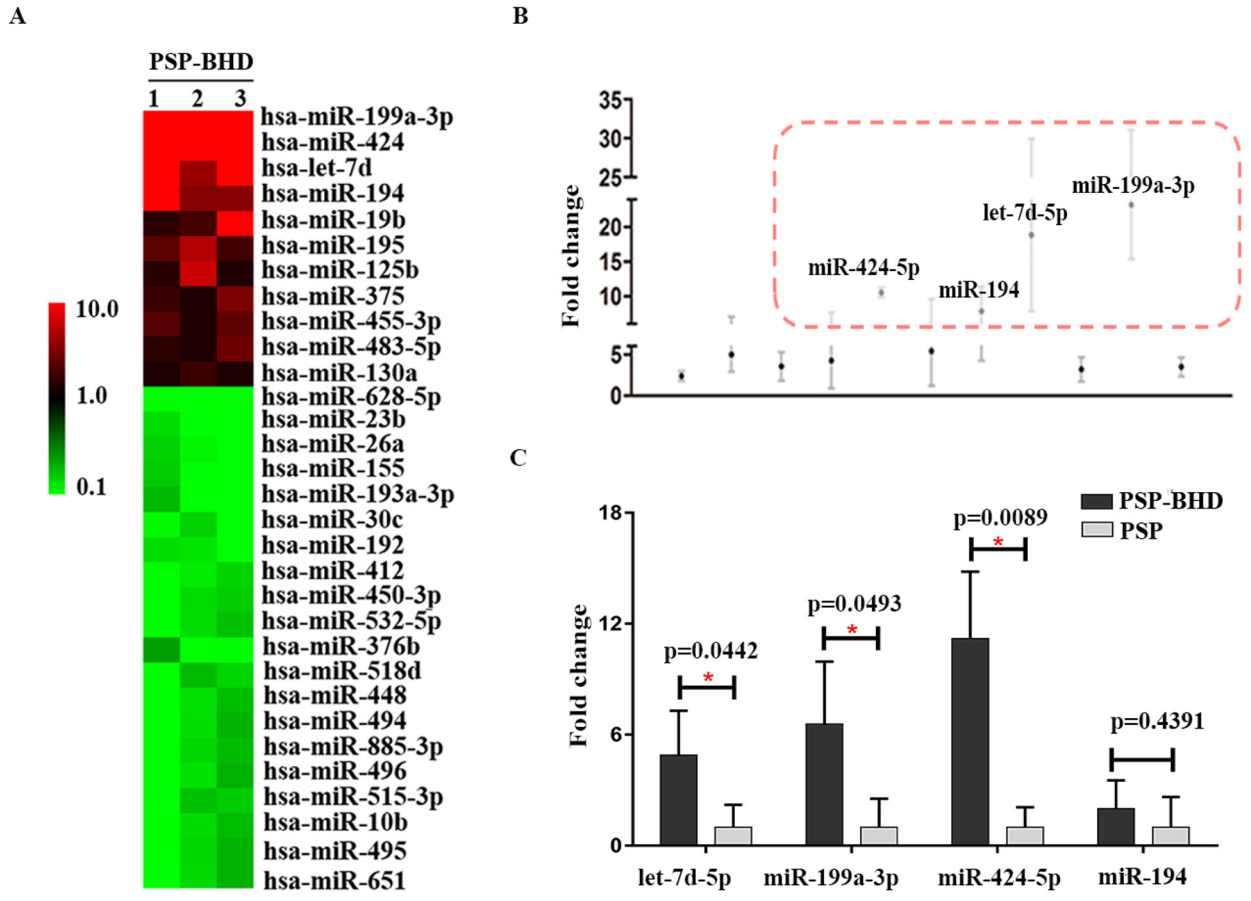

Figure 1 miRNA signature uncovered in BHD cystic lesions. (A) Represented miRNAs dysregulated in cystic lesions of PSP-BHD (n=3) compared to that of PSP (n=3) patients. Mutations of FLCN gene are p.(P63TfsX69), p.(S316YfsX73) and p.(Arg527GlnfsX75). (B) Four miRNAs were found fivefold or more increase in PSP-BHD in microarray analysis. (C) Increases of miR-424-5p, let-7d-5p and miR-199a-3p were confirmed in cystic lesions of PSP-BHD (n=14) compared to that of PSP patients (n=14). The mutation information of PSP-BHD patients was in online supplementary table 1. The columns represent mean and the bars indicate SD. BHD, Birt-Hogg-Dubé syndrome; FLCN, folliculin; miRNA, microRNA; PSP, primary spontaneous pneumothorax. * Represents statistical significance.

mechanism.[12 13] However, in FLCN study, the involvement of miRNAs in the pathogenesis of pulmonary cysts in BHDS is under studied. Nevertheless, the characteristic histology of the lung lesions of BHDS exhibits no obvious inflammation and reparative response,[14] implicating a suppressive nature of FLCN deficiency on the mesenchyme that is essential in damage-related tissue repairing. On the other hand, in a mouse model of FLCN-null in lung type II alveolar epithelial cells, an increased epithelial apoptosis is detected.[15] These observations indicate an involvement of epithelial damage and mesenchymal suppression, however, no cystic lesions are ever induced experimentally. Thus, the molecular mechanism that may explain lesion pathology of PSP-BHD deserves a systematic exploration.

Herein, we sought to identify miRNAs differentially expressed in PSP-BHD and PSP patients for a diagnostic application and for elucidating the molecular mechanisms of these miRNAs in the pathogenesis of the disease.

METHODS

Population

PSP patients admitted according to the guidelines of the British Thoracic Society[16] and normal controls (NCs) were enrolled to Department of Cardiothoracic Surgery of Taizhou Hospital of Zhejiang Province and Nanjing Chest Hospital between 2006 and 2015.

Cell lines

Human bronchial epithelial cells (BEAS-2B), human lung epithelial A549 cells, human keratinocyte cells (HaCaT), human embryonic lung fibroblasts (HELF) and human embryonic kidney cells (HEK293) were purchased from China Center for Type Culture Collection.

miRNAs assay, quantitative PCR analysis and Western blot

For miRNAs screen, Universal Probe Library assays (Roche) were used. For miRNA/mRNA or protein detection, RT-qPCR or western blot (WB) was used, respectively.

Apoptosis detection

Apoptosis in cultured cells was analysed by AnnexinV-FITC and propidium iodide staining using a calibur flow cytometer (BD Biosciences). Apoptosis in the lung tissues was analysed with TdT-mediated dUTP Nick-End Labeling (TUNEL) assays using in situ Cell Death Detection Fluorescein Kit (Roche).

Luciferase reporter construction and assay

The target sequences of Smad7 and Frizzled 4 (FZD4) 3′-Untranslated Region (3′ UTR) were amplified and subcloned (Realgene) into a dual-luciferase reporter vector (Promega), respectively. The luciferase reporter assays were performed in HEK293 cells.

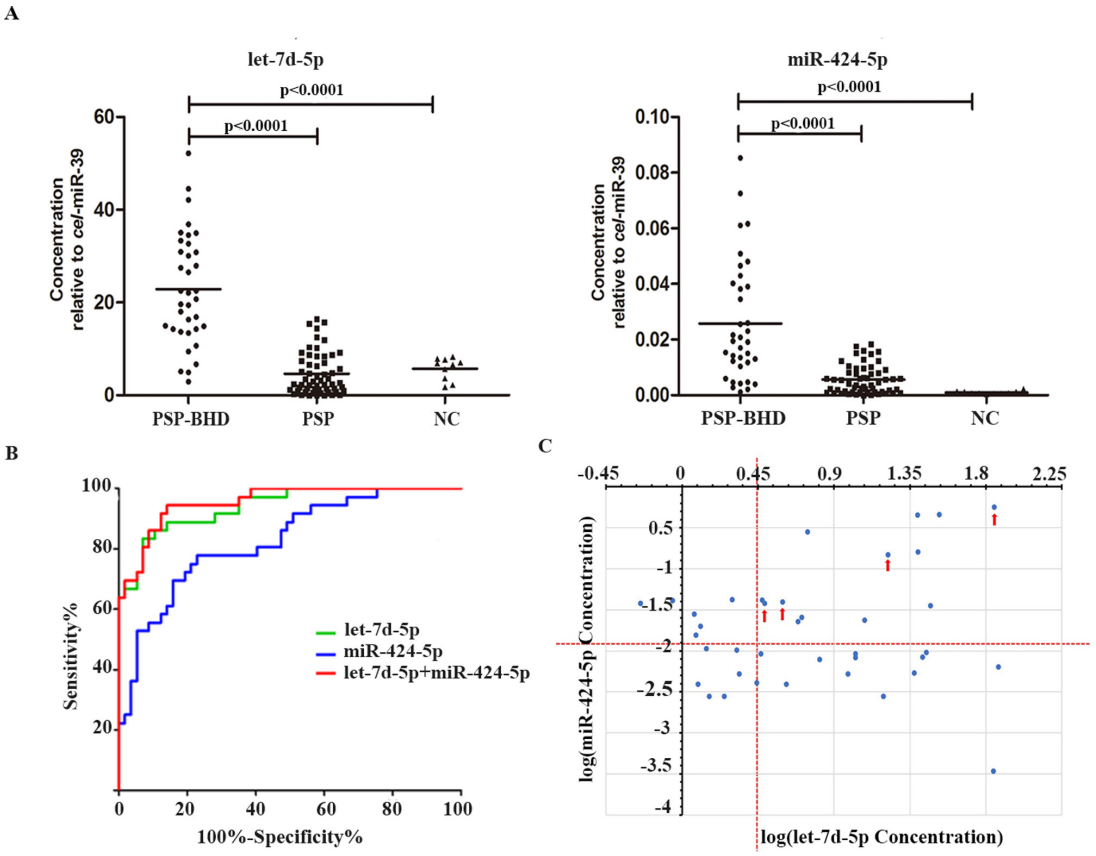

Figure 2 Plasma miR-424-5p and let-7d-5p differentially diagnosed PSP-BHD from PSP. (A) The relative concentration of miR-424-5p and let-7d-5p to cel-miR-39 in plasma of PSP-BHD patients (n=36), PSP patients (n=57) and normal controls (NCs) (n=15). NC represents normal controls. The dashes represent the mean values. A stepwise linear regression by SPSS V.17.0 was used to conclude that FLAN mutation was a major contributor to the expressions of miR-424-5p and let-7d-5p (online supplementary table 3). (B) ROC curves of plasma detections as signal or combined biomarkers. (C) The relative concentrations of miR-424–5p and let-7d-5p to cel-miR-39 in plasma of PSP population (n=38) of the prospective study. The red dotted lines are the cut-off values of miR-424–5 p and let-7d-5p. The red arrows indicated BHDS patients confirmed by genetic analysis. BHD, Birt-Hogg-Dubé syndrome; FLCN, folliculin; PSP, primary spontaneous pneumothorax; ROC, receiver operating characteristic.

Immunohistochemistry and H&E staining

Tissues were fixed in 4% paraformaldehyde and embedded in paraffin. Tissue sections (7 µm) were prepared for immunohistochemistry of Smad7, FZD4, Vimentin, α-smooth muscle actin (α-SMA), tight junction protein 1 (TJP1) and Snail, and for H&E staining.

Data analysis and statistics

Receiver operator characteristic (ROC) curves were generated by plotting Sensitivity% versus (100%-specificity%) and the areas under the curves (AUCs) were calculated. Logistic regression analysis was used for the evaluation of the accuracy of combined miRNA markers. For WB and wound-healing experiments data quantified by ImageJ, and for qPCR data of miRNA/mRNA levels, Student's t-test was used. For plasma miRNA levels, Tukey's test followed by Duncan's multiple range test was used. All statistical analyses were performed with either SPSS V.17.0 or GraphPad Prism V.5.0 Software (quantifying uncertainty of 95% CIs and statistical significance of $p<0.05$) and all p values of comparisons were detailed in online supplementary files.

The details of the methods were provided in online supplementary methods.

Table 1 Diagnostic accuracies of measurements of single markers for predicting PSP-BHD at predefined specificities and sensitivities

	AUC (95% CI)	Sensitivity at 90%: specificity, %	Sensitivity at 90%, specificity, %:
let-7d-5p	0.93 (0.88 to 0.99)	73.1	82.1
miR-424–5p	0.87 (0.79 to 0.95)	58	64.3
let-7d-5p+miR-424–5p	0.96 (0.92 to 1.00)	90.4	92.9

AUC, area under the curve; BHD, Birt-Hogg-Dubé syndrome; PSP, primary spontaneous pneumothorax.

RESULTS

miRNA signature uncovered in BHDS cystic lesions

We initially compared the expression profiles of miRNAs in cystic lesions of PSP-BHD patients to that of PSP patients (n=3, respectively) via a commercialised microarray (Roche). Totally, 11 upregulated and 52 downregulated miRNAs were uncovered in the cystic tissues of PSP-BHD patients when compared with that of PSPs (figure 1A and see online supplementary table 4). Wingless/ integrated (WNT), transforming growth factor-β (TGF-β), epidermal growth factor receptor (ErbB), mitogen-activated protein kinase (MAPK), phosphatidylinositol 3' –kinase (PI3K)-Akt (PI3K-Akt) and mammalian target of rapamycin (mTOR) signalling pathways were targeted by these miRNAs on DIANA-miRPath V.2.0 prediction[17 18] (see online supplementary

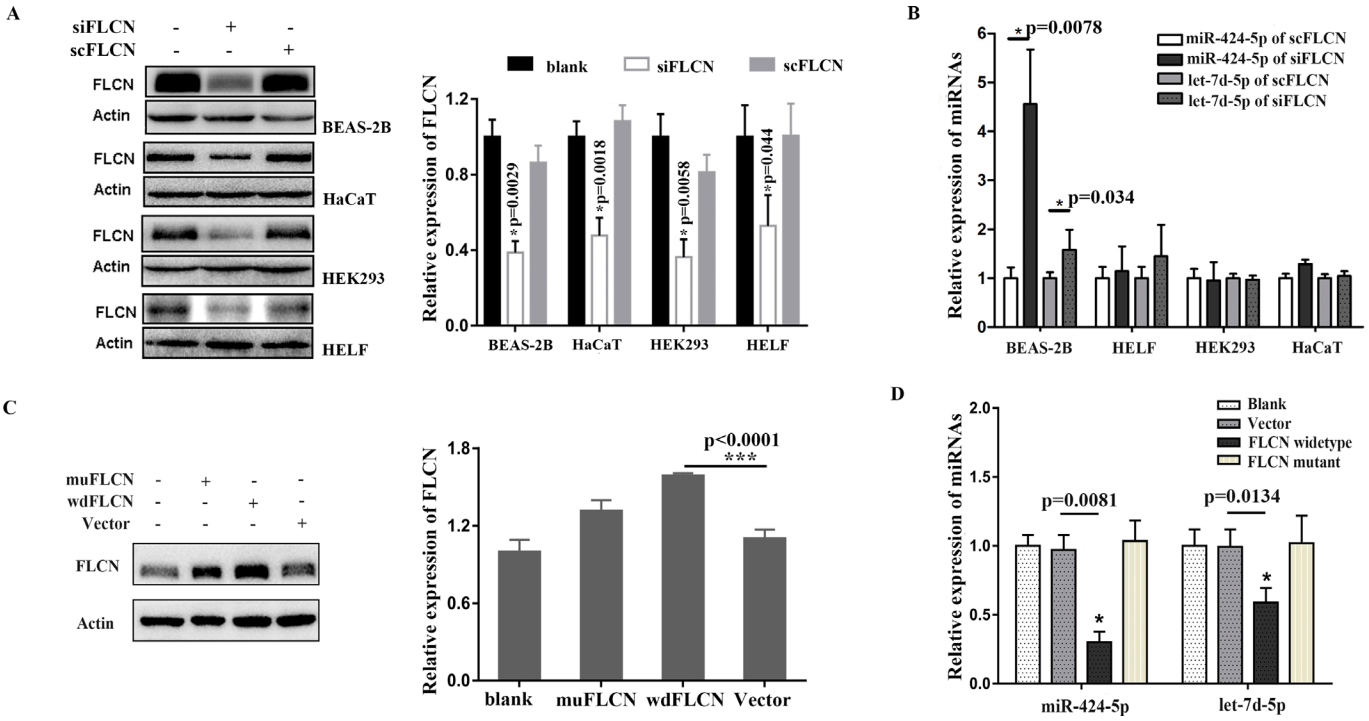

Figure 3 FLCN suppressed miR-424-5p and let-7d-5p expressions in lung epithelial cells. (A) Endogenous FLCN was knockdown by siRNA in different cell lines and was statistically calculated with four times experiments. (B) The expression of miR-424-5p and let-7d-5p in different cells with FLCN knockdown. siFLCN means a siRNA sequence of FLCN, scFLCN means a scramble sequence of FLCN. (C) Protein expression of FLCN in A549 cells with widetype-FLCN-expressed plasmids (wdFLCN), mutant-FLCN expressed plasmids (muFLCN) and blank vectors and was statistically calculated with four times experiments. FLCN mutant was p.(Arg527Glnfs*75). (D) The expression of miR-424-5p and let-7d-5p in A549 cells with wdFLCN, muFLCN and vectors. The columns represent mean and the bars indicate SD. FLCN, Folliculin.

table 5). Since downregulated miRNA may not be ideal as biomarker for diagnosis, four upregulated miRNAs with fivefold or more increase in PSP-BHD patients, including miR-424–5p, let-7d-5p, miR-199a-3p and miR-194, were arbitrary chosen for subsequent studies (figure 1B). In an expanded collection of PSP-BHD and an equal number of PSP lesion samples (n=14), the expressions of miR-424–5 p, miR-199a-3p and let-7d-5p were confirmed to be increased in PSP-BHD with 10-fold, 6.6-fold and 4.9-fold changes, respectively, when compared with those of PSP (figure 1C). Thus, PSP-BHD cystic lesion exhibited specific miRNA signature.

Plasma miR-424-5p and let-7d-5p differentially diagnosed PSP-BHD from PSP

To determine whether the upregulated miRNAs in the cystic lesion may appropriately serve as biomarkers for differential diagnosis between PSP-BHD and PSP, the relative levels of the three miRNAs were determined in the plasma of 36 PSP-BHD and 57 PSP patients, as well as 15 NC. As expected, miR-424–5p and let-7d-5p were significantly higher in PSP-BHD patients compared with those of PSP and NC individuals (figure 2A). However, the relative concentration of miR-199a-3p in PSP-BHD plasma was equivalent to that of NC, but obviously reduced in PSP patients (see online supplementary figure S1), thus, resulted in the selection of miR-199a-3p in the initial screen.

Next, the ROC curves were constructed by comparing plasma measurements of the identified miRNAs in PSP-BHD and PSP groups. The AUCs were calculated. The single AUC of miR-424–5p or let-7d-5p was 0.87 or 0.93, respectively, and the AUC of the two combined was improved to 0.96 (figure 2C and table 1). The sensitivity at the fixed specificity of 90% of the combination were also improved and vice versa (table 1). The cut-off values of miR-424–5 p and let-7d-5p calculated on Yuden index were 0.0116 and 2.839 that resulted in 100% sensitivity and 62% specificity. Using these values, we screened a cohort of 38 genetically undefined PSP patients with blind of any additional clinical information. A total 13 candidates for BHDS were suggested and 4 of them (31%) were eventually confirmed to be FLCN-mutation carriers by genetic examinations. None of the rest 25 PSP patients was FLCN-mutation carrier (figure 2C). Thus, the miRNA screen cut down about 2/3 (65.8%) genetic analysis of FLCN that is largely unavailable in local clinics.

FLCN negatively regulated miR-424-5p and let-7d-5p in lung epithelial cells

Subsequently, a set of human cell lines with different origins including the lung epithelial cell BEAS-2B, embryonic lung fibroblast HELF, skin epithelial cell HaCaT and embryonic kidney cell HEK293 were prepared for FLCN knockdown studies (figure 3A). On FLCN disruption, the expressions of miR-424–5p and let-7d-5p were significantly increased only in BEAS-2B cells (figure 3B), suggesting a cell-specific regulation of the two by FLCN. In consistent, in a lung epithelial cell line A549 with low endogenous FLCN (figure 3C), the ectopic expression of a wild type FLCN gene resulted in a significant downregulation of miR-424–5p and let-7d-5p. In contrast, a disease-causing mutation (p.(Arg527Glnfs*75))[19] deprived this suppressive function of FLCN (figure 3D). Thus, FLCN specifically and negatively regulated miR-424–5 p and let-7d-5p in lung epithelial cells.

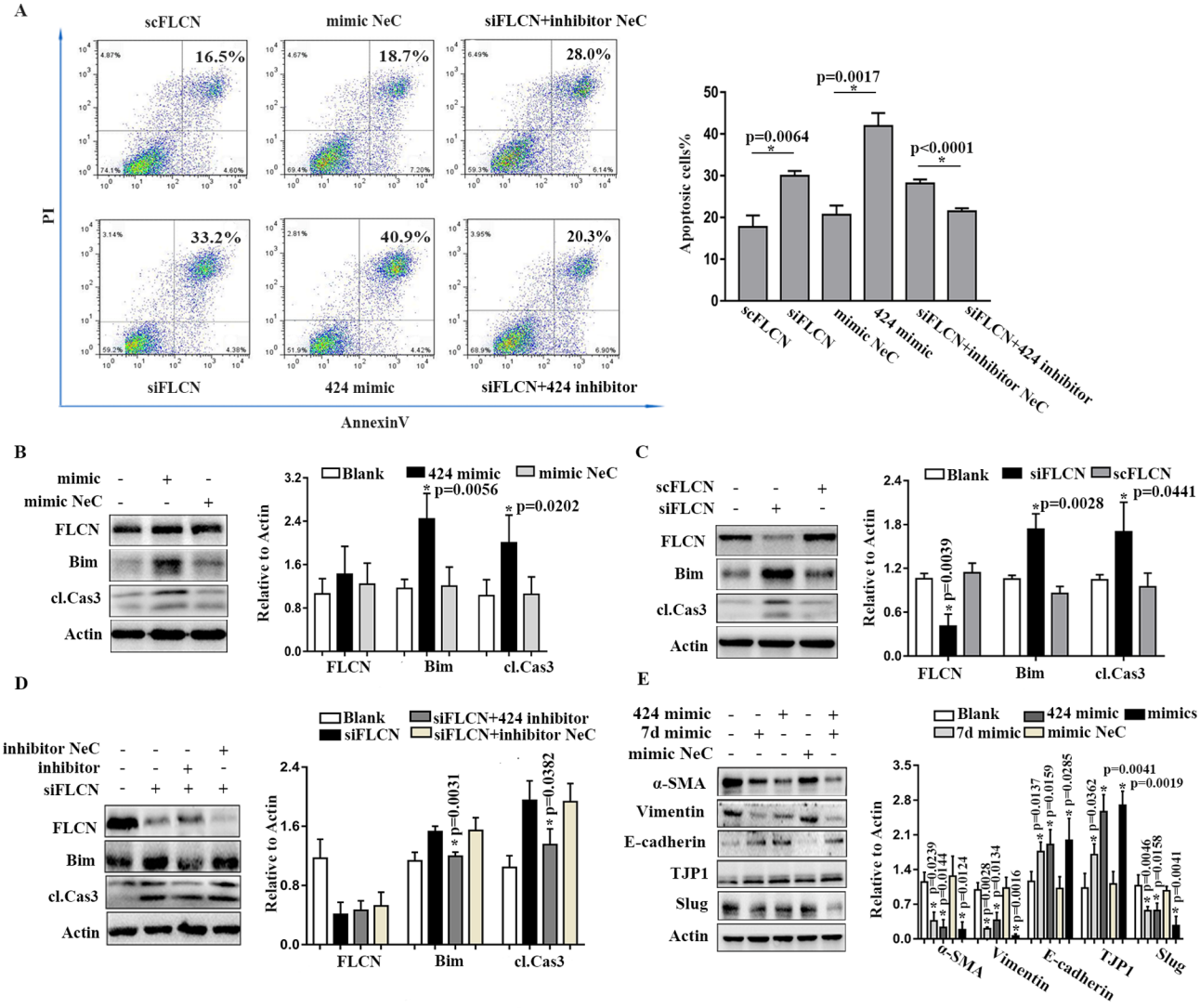

Figure 4 FLCN-regulated miRNAs exhibited cell-specific functions. (A) Apoptosis of BEAS-2B cells was increased with FLCN interference or miR-424-5p mimic, respectively, and miR-424-5p inhibitor blocked the apoptosis of BEAS-2B cells induced by FLCN interference by FACS analysis with statistical calculation. (B, C) Bim and Cleaved Caspase3 (cl.Cas3) were upregulated with miR-424-5p mimic (B) or FLCN interference (C) with statistical calculation. P values were calculated by comparing with mimic NeC (B) or scFLCN (C). (D) The upregulation of Bim and cl.Cas3 induced by FLCN knockdown were blocked by miR-424-5p inhibitor in BEAS2B cells with statistical calculation. P values were calculated by comparing with inhibitor NeC. (E) Proteins of vimentin, α-SMA and Slug were reduced significantly while TJP1 and E-Cadherin were increased in HELF cells with miR-424-5p and/or let-7d-5p mimics with statistical calculation. 424 represents miR-424-5p and 7d represents let-7d-5p. The columns of B–E represent mean of the relative expression and the bars indicate SD of the triplicate experiments. FLCN, folliculin; scFLCN, sequence of FLCN.

FLCN-regulated miRNAs exhibited cell-specific functions

Next, we studied the functions of FLCN-regulated miRNAs in cells with different origins by introducing miR-424–5p and/or let-7d-5p mimics. Only miR-424–5p mimics in BEAS-2B cells induced apoptosis (figure 4A) with increased expressions of Bim and cleaved Caspase3 (cl.Cas3) (figure 4B). Consistently, FLCN knockdown also induced apoptosis in BEAS-2B, but not HaCaT, HELF or HEK293 cells, along with increased Bim and cl.Cas3 (figure 4A,C and see online supplementary figure S2). And, an inhibitor of miR-424–5p suppressed this effect of FLCN knockdown (figure 4A,D).

In lung fibroblast HELF, the introduction of miR-424–5p/let-7d-5p mimics potently induced a mesenchymal–epithelial transition (MET) revealed by significant reduction of fibroblastic marker vimentin, α-SMA and Slug, and increase of epithelial indicator TJP1 and E-Cadherin both at mRNA and protein levels (figure 4E and see online supplementary figure S3). No obvious changes of these indicators were observed in HELF cells with FLCN knockdown (see online supplementary figure S2), suggesting that the introduction of miR-424–5p/let-7d-5p was necessary and sufficient for the induction of MET in HELF cells. We did not observe any of MET response in HaCaT or HEK293 cells by miR-424–5p/let-7d-5p (data not shown). Importantly, miR-424–5p/let-7d-5p mimics induced specific cell responses, apoptosis or MET, in FLCN knockdown BEAS-2B or HELF cells, respectively, at an equal potency as in non-FLCN knockdown BEAS-2B or HELF cells (see online supplementary figure S4).

Cell-pecific function of the miRNAs targeted TGF-β or WNT pathway

To elucidate the signalling mechanisms underlying the functions of miR-424–5p and let-7d-5p, we analysed the targets of the two

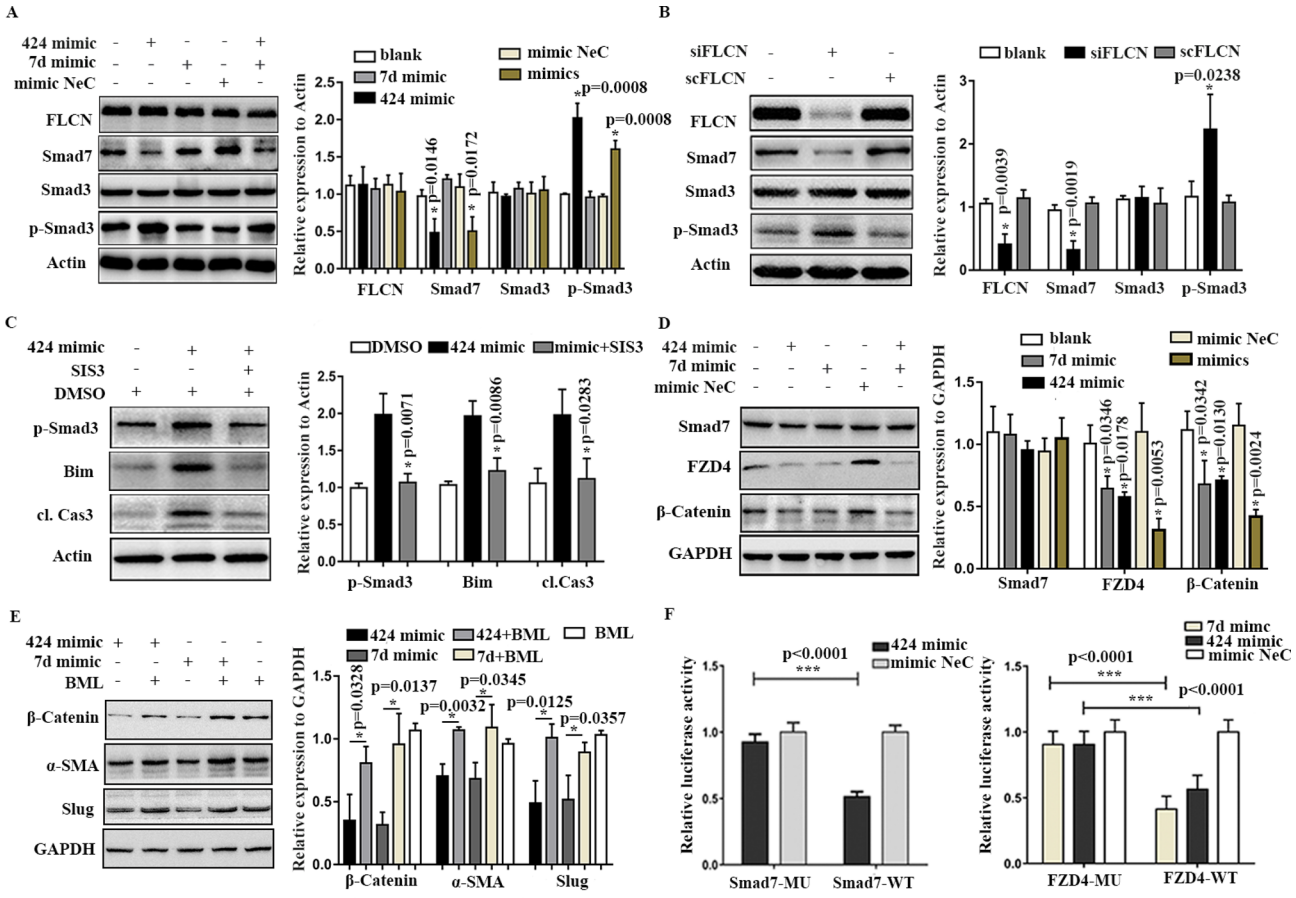

Figure 5 Smad7 was targeted by miR-424-5p and FZD4 was targeted by both miR-424-5p and let-7d-5p. (A, B) Smad7 was suppressed and p-Smad3 was activated in BEAS-2B cells with miR-424-5p mimic (A) or FLCN knockdown (B) and was statistically analysed. (C) Inhibition of p-Smad3 by SIS3 suppressed the upregulation of Bim and cl.Cas3 with miR-424-5p mimic and was statistically analysed. (D) FZD4 and βcatenin were downregulated with miR-424-5p or/and let-7d-5p mimics and was statistically analysed. (E) Activation of β-Catenin by BML restored the suppression of α-SMA and Slug expression with miR-424-5p or let-7d-5p mimic and was statistically analysed. (F) The relative luciferase activity of Smad7 wildtype vectors was suppressed by miR-424-5p mimic and the relative luciferase activity of FZD4 wildtype vectors was suppressed by both miR-424-5p and let-7d-5p mimics with statistical significance. 424 represents miR-424- 5p and 7d represents let-7d-5p. The columns in the figure represent mean of the relative expression and the bars indicate SD with triplicate experiments. cl.Cas3, cleaved Caspase3; FLCN, folliculin; scFLCN, scramble sequence of FLCN; siFLCN, sequence of FLCN.

through DIANA-miRPath V.2.0. Interestingly, three pathways (WNT, TGF-β and mTOR pathways) were prominent in the prediction, which intersected the initial results uncovered in the microarray analysis (see online supplementary tables 5 and 6). Six candidates (see online supplementary table 6) in these pathways with higher affinity scores were chosen for further analysis. In BEAS-2B cells, only Smad7, a TGF-β signalling component, was significantly suppressed by miR-424–5p mimics or FLCN knockdown, and the phosphorylation of its downstream Smad3 (p-Smad3) was largely increased (figure 5A,B). miR-424–5p in FLCN disrupted BEAS-2B cells showed similar results (see online supplementary figure S4). Importantly, a p-Smad3 inhibitor SIS3[20] blocked Bim and Caspase 3 activation induced by miR-424–5p (figure 5C), indicating that miR-424–5p targeted TGF-β signalling is functionally crucial and cellular specific. Finally, the mimics of let-7d-5p showed no detectable effect of any on BEAS-2B cells.

In HELF cells both miR-424–5p and let-7d-5p mimics suppressed WNT signalling receptor FZD4. Accordingly, its downstream component β-Catenin was down-regulated (figure 5D). Whereas, an activator of β-Catenin[21] reversed the effect of both miR-424–5p and let-7d-5p mimics on induction of MET in HELF cells (figure 5E). Noted of, FLCN knockdown alone in HELF cells did not show WNT signalling disruption (see online supplementary figure S2), yet both miR-424–5p and let-7d-5p mimics did, and importantly, both mimics worked in the condition of FLCN knockdown (see online supplementary figure S4). Together, miR-424–5p, as well as let-7d-5p mimics delivered different functions on the origin of cells by targeting either TGF-β or WNT pathway. No change of mTOR signalling was detected in BEAS-2B or HELF cells (data not shown) on the introduction of miR-424–5p and let-7d-5p mimics.

Finally, the sequence specificity that targeted miR-424–5p to Smad7 3'UTR at the predicted position 55, and miR-424–5p/let-7d-5p to FZD4 3'UTR at the position 712 and 5028 were confirmed by relative luciferase activity assay (figure 5F) using the reporter constructs that cloned the corresponding miRNAs' target sequences (see online supplementary figure S6) in human embryonic kidney cell HEK293, a cell system commonly used for testing miRNA sequence specificity and function. Thus, TGF-β and WNT pathways were regulated by the miRNAs in a cell specific manner (see online supplementary figure S7). miRNAs suppressed cellular reparative response via TGF-β and WNT signalling.

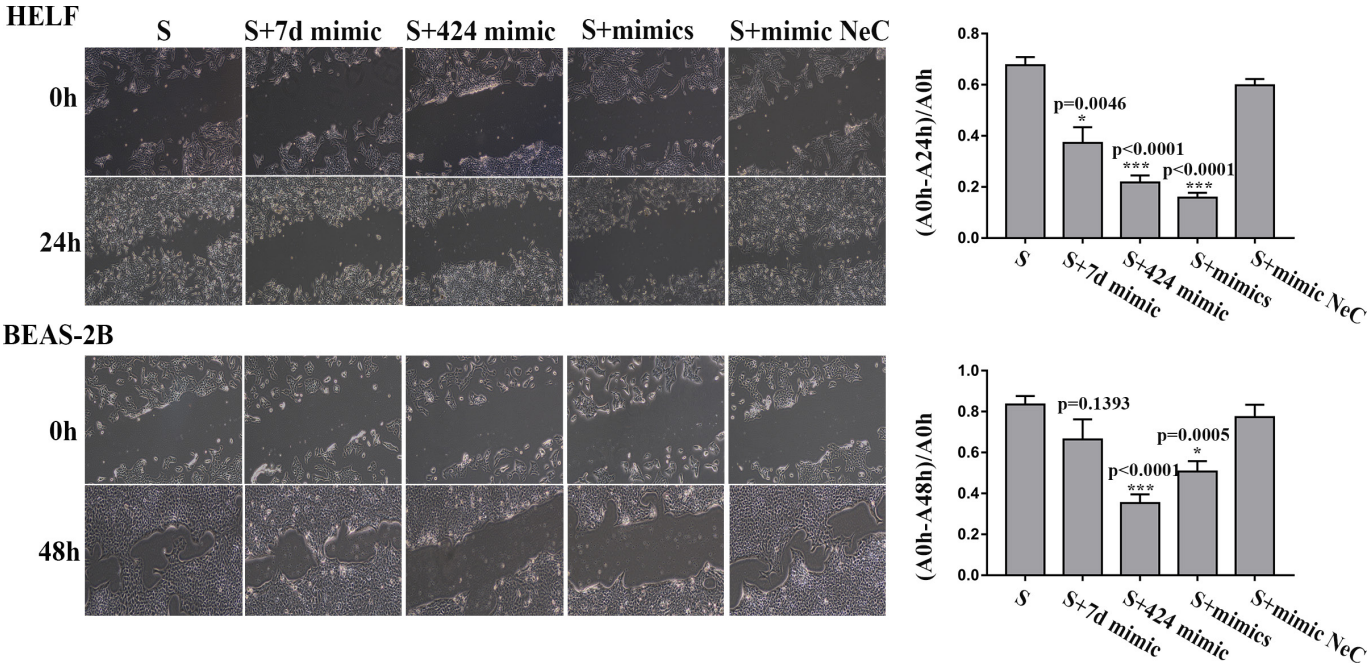

Figure 6 Cellular wound-healing responses were suppressed by miR-424-5p or let-7d-5p. (left) Representative pictures of scratch experiments in HELF and BEAS-2B cells with miR-424-5p or/and let-7d-5p mimics. (right) Growth rate of wounded HELF and BEAS-2B cells with miR-424-5p or/and let-7d-5p mimics with at least triplicate experiments. The columns represent the means and the bars indicate SE of the means with triplicates. S represents scratch, 7d means has-let-7d-5p, 424 means has-miR-424-5p and NeC represents negative control. A0h means the area of scratch at the time of the scratch treatment, A24h means the area of scratch at the time of 24 hours later after the scratch treatment, A48h means the area of scratch at the time of 48 hours later after the scratch treatment.

To test the role of FLCN-regulated miRNAs in cellular repairing, a process involving both TGF-β and WNT signaling,[22 23] we assayed cell responses to harmful stress with/without the treatment of the miRNAs mimics. In HELF cells, the scratch significantly triggered wound-healing response along the edge of damage (figure 6). Moreover, it induced α-SMA expression in the insulted cells (see online supplementary figure S8), indicating an effective initiation of mesenchymal cellular reparative response and its molecular adaptation. In contrast, the administration of miR-424–5p/let-7d-5p strongly suppressed this process (figure 6 and see online supplementary figure S8). Consistently, in BEAS-2B cells, a typical epithelial cellular reparative response was also initiated on scratch and specified by cell growth and EMT response with α-SMA and Slug activation and E-Cadherin reduction, which was strongly suppressed by miR-424–5p, but not let-7d-5p mimics (figure 6 and see online supplementary figure S8). The effect of the two miRNAs on wound-healing response in HELF and BEAS-2B cells were repeatable in the condition of FLCN knockdown (see online supplementary figure S9 and 10). Thus, FLCN-regulated miRNAs appeared suppressive in cellular reparative response after injury.

Evidence for loss of cellular reparative response was detected in PSP-BHD lesions

Finally, we validated the above cellular observations in the cystic tissues of PSP-BHD patients. As shown, a suppression of Smad7 and an activation of Smad3, as well as a decrease of FZD4 and β-catenin in the PSP-BHD cystic tissues were evident (figure 7A,C,F), suggesting an activation of TGF-β and a suppression of WNT signalling in PSP-BHD lung lesions, which was consistent with the cellular findings. Moreover, the protein levels of Bim and cl.Cas3 were significantly increased (figure 7B) and TUNEL assay detected an increased cell apoptosis in the lesion tissues (figure 7E). Moreover, an epithelial marker TJP1 was increased, while the mesenchymal indicator vimentin, α-SMA and Slug were decreased in PSP-BHD lung lesions (figure 7F), indicating an MET molecular adaptation that was initially revealed in the cell studies.

To show more definitively that an overall tissue EMT configuration in the lesions of PSP-BHD tissues indeed related to the suppression of cellular reparative response, we set an immunohistochemistry study around the cystic regions. When compared with NCs, in PSP tissues, the expression of α-SMA was greatly increased in a broadly distributed cells around lesion areas, whereas, the expression of TJP1 was obviously reduced in the epithelial cells (figure 7F), suggesting that given the extent of the tissue damage around cysts, the cellular reparative response was induced. However, in PSP-BHD lesions, an opposite staining pattern with greatly reduced α-SMA and increased TJP1 was detected (figure 7F). Together, a loss of cellular reparative response in PSP-BHD lung lesions was suggested.

DISCUSSION

Spontaneous pneumothorax shared between BHDS and PSP[24–27] is often the first presenting manifestation[28] and may be the only one of BHDS,[29–31] whereas, the skin findings generally appear in the fourth decade of FLCN mutant carriers and become progressively more noticeable with age.[32–34] The renal phenotype of BHDS is also a late finding when compared with pulmonary cysts/pneumothorax.[6 35] Thus, the PSP-BHD is a forme fruste type of the disease,[36] which may confuse precise diagnosis with PSP. In fact, our previous studies and others' find[2 26 29 30] that spontaneous pneumothorax is the most frequently reported clinical manifestation of PSP-BHDS patients enrolled in the thoracic surgery, occupied as much as 10% of 'PSP' population.

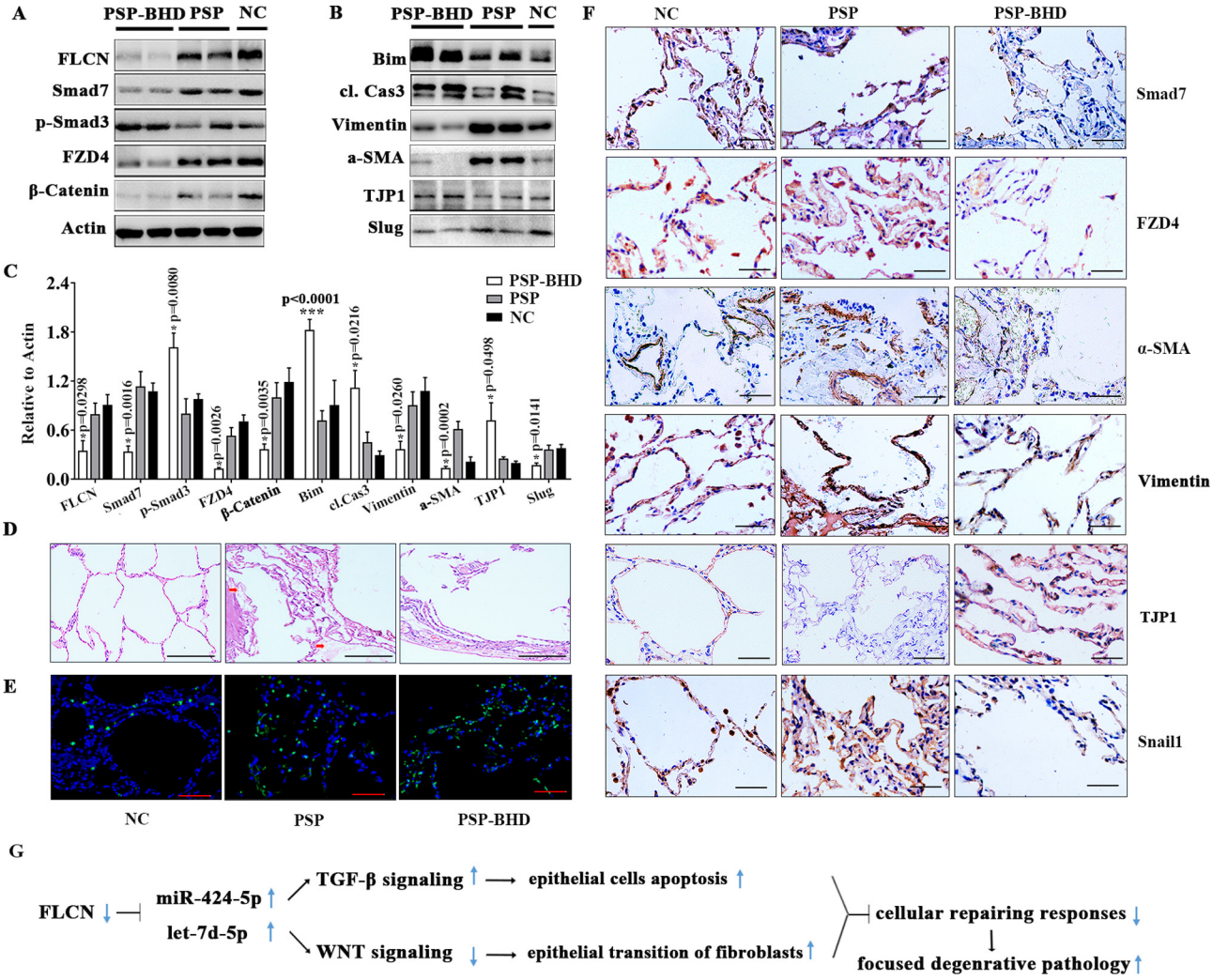

Figure 7 Evidence for cell death and loss of cellular reparative responses in PSP-BHD lesion. (A) Proteins of TGF-β signalling activated and WNT signalling suppressed in cystic lesions of PSP-BHD patients compared to PSP patients and cancer-free tissues (NC) lung tissues. (B) Proteins of Bim, cl.Cas3 and TJP1 upregulated and vimentin and a-SMA downregulated in cystic lesions of PSP-BHD patients compared to PSP patients and controls. (C) Quantitation of proteins observed in A and B (PSP-BHD n=15, PSP n=15, NC n=9). The columns represent the means and the bars indicate standard deviation. The mutation information of PSP-BHD patients was in online supplementary table 1. (D) HE staining of lung tissue of PSP-BHD patients, PSP patients and NC. The red rows indicated exudation of the tissue. (E) Increased apoptosis observed by TUNEL in tissue section of PSP-BHD compared with that of PSP and NC. (F) Smad7, FZD4, vimentin, α-SMA and Snail1 were all suppressed while TJP1 was enhanced in lesion tissue of PSP-BHD patient compared with that of PSP and NC by immunochemistry. (E) A model of cystic formation in PSP-BHD lung. The black star showed exudation. The blank line indicated 100 μm and the red line indicated 50 μm. BHD, cICas 3, cleaved caspase 3; FLCN, folliculin; NC, normal control; PSP, primary spontaneous pneumothorax; TGF-β, transforming growth factor-β;

Thus, developing a new and cost-effective diagnostic approach for large population screen of PSP-BHD, in addition to classic genetic examination, is desirable.

In this study, we found that PSP-BHD patients showed specific miRNAs profiles compared with PSP suffers in cystic lesion and circulation, characterised by a significant and robust increase of miR-424–5p and let-7d-5p. The combination of the two delivered high diagnostic accuracy with the sensitivity at the fixed specificity of 90%. Using the combined marker, we predicted the BHDS cases in a prospective study with narrowing PSP population to 1/3 for further genetic analysis that is often central technically, unavailable for most local hospitals at least in developing regions, and costly for a large population screen. Our concept-proof study argued that miRNA detection as an initial screen may be valuable when a Mendelian syndrome with an atypical manifestation that needs to be differentiated from other conditions that pose similar clinic appearance before a genetic analysis.

Furthermore, we also showed that miR-424–5p and let-7d-5p provided important tools in elucidating the nature of BHDS' lung pathology. Previously, studies on FLCN function revealed that BHD lungs had an increased alveolar epithelial cell apoptosis in animals and humans.[15] We further showed that the increased apoptosis of lung epithelial cells directly linked to the function of miR-424–5 p that reduced Smad7 and enhanced Smad 3 signalling. In contrast, both miR-424–5p and let-7d-5p forced a cellular adaptation of MET via the suppression of WNT signalling in lung fibroblasts. Considering that both BEAS-2B and HELF cells expressed Smad7 and FZD4 (figure 5B and see online supplementary figure S2 and 4), as well as other tested components of WNT, TGF-β and mTOR pathways, the miRNAs exhibited selective targeting powers in different cells with yet unknown mechanism.

Tissue studies revealed a similar molecular alteration in the BHDS lung lesions with a TGF-β pathway activation and WNT signalling suppression. Importantly, given the extent of the lung lesion in BHDS, no reparative response was detected, instead, both normal tissue repair index EMT and myofibroblast activation[22 23] were suppressed, distinguishing with non-BHDS PSP lesions that showed obvious repairing adaptation both at molecular and immunohistochemistry levels. Thus, an increased epithelium apoptosis and a weakened mesenchyme repairing may define a pathogenic condition that contributes to the development of focused degenerative cystic lesions in BHD lungs (figure 7G).

The mechanism of how FLCN might negatively regulate the miRNAs is still not known. However, a recent study shows that FLCN knockdown inhibits the motility and perinuclear clustering of lysosome,[37] which alters the cellular function of lysosome by increasing its PH.[38] Interestingly, a similar change in lysosome has been linked to the increase of exosomal secretion in cells,[39] indicating that FLCN deficiency may involve in hypersecretion of miRNAs, presumably in lung epithelial cells. More studies are required to deepen the mechanistic understanding of FLCN in BHDS pathology. Finally, it is acknowledged that p values of several experiments raised the possibility of type I errors (false positive), specifically in the comparisons of miR-199a-3p expression between PSP-BHD and PSP ($p=0.0493$) and the expression of TJP1 protein (PSP-BHD vs PSP, $p=0.0498$) in lung tissues (see online supplementary table 7), which may suggest the necessity for the further validation in an expanded cohort in future.

Author affiliations
[1]Jiangsu Key Laboratory for Molecular Medicine, Nanjing University Medical School, Nanjing, Jiangsu, China
[2]Center for Translational Medicine, Nanjing University Medical School, Nanjing, Jiangsu, China
[3]Department of Cardiothoracic Surgery, Taizhou Hospital of Zhejiang Province, Wenzhou Medical University, Linhai, Zhejiang, China
[4]Department of Thoracic Surgery, Nanjing Chest Hospital, Nanjing, Jiangsu, China
[5]Department of Pathology, Nanjing Chest Hospital, Nanjing, Jiangsu, China

Acknowledgements We would like to thank all the PSP patients and their family members who participated in the studies and the staff of Human Tissue Bank of Taizhou Hospital of Zhejiang Province for their contributions. We also thank Xicong Zhu, dermatologist at Taizhou Hospital, for dermatological examination, and candidates Lingjia Zhuang and Yu Zhang for tissue section scores.

Funding The study was supported by the National Natural Science Foundation of China (81570775 and 81670003), and National Key R&D Program of China (2018YFC2001800).

Competing interests None declared.

Patient consent for publication Not required.

Ethics approval The study was approved by the ethics committee of the two hospitals.

Provenance and peer review Not commissioned; externally peer reviewed.

Data availability statement Data are available in a public, open access repository.

ORCID iD
Qian Gao http://orcid.org/0000-0001-8189-6061

REFERENCES

1 Nickerson ML, Warren MB, Toro JR, *et al*. Mutations in a novel gene lead to kidney tumors, lung wall defects, and benign tumors of the hair follicle in patients with the Birt-Hogg-Dubé syndrome. *Cancer Cell* 2002;2:157–64.
2 Ren H-Z, Zhu C-C, Yang C, *et al*. Mutation analysis of the FLCN gene in Chinese patients with sporadic and familial isolated primary spontaneous pneumothorax. *Clin Genet* 2008;74:178–83.
3 Painter JN, Tapanainen H, Somer M, *et al*. A 4-bp deletion in the Birt-Hogg-Dubé gene (FLCN) causes dominantly inherited spontaneous pneumothorax. *Am J Hum Genet* 2005;76:522–7.
4 Kunogi M, Kurihara M, Ikegami TS, *et al*. Clinical and genetic spectrum of Birt-Hogg-Dube syndrome patients in whom pneumothorax and/or multiple lung cysts are the presenting feature. *J Med Genet* 2010;47:281–7.
5 Zbar B, Alvord WG, Glenn G, *et al*. Risk of renal and colonic neoplasms and spontaneous pneumothorax in the Birt-Hogg-Dubé syndrome. *Cancer Epidemiol Biomarkers Prev* 2002;11:393–400.
6 Houweling AC, Gijezen LM, Jonker MA, *et al*. Renal cancer and pneumothorax risk in Birt-Hogg-Dubé syndrome; an analysis of 115 FLCN mutation carriers from 35 BHD families. *Br J Cancer* 2011;105:1912–9.
7 Toro JR, Wei M-H, Glenn GM, *et al*. BHD mutations, clinical and molecular genetic investigations of Birt-Hogg-Dubé syndrome: a new series of 50 families and a review of published reports. *J Med Genet* 2008;45:321–31.
8 Menko FH, van Steensel MAM, Giraud S, *et al*. Birt-Hogg-Dubé syndrome: diagnosis and management. *Lancet Oncol* 2009;10:1199–206.
9 Cacchiarelli D, Legnini I, Martone J, *et al*. miRNAs as serum biomarkers for Duchenne muscular dystrophy. *EMBO Mol Med* 2011;3:258–65.
10 Liu R, Chen X, Du Y, *et al*. Serum microRNA expression profile as a biomarker in the diagnosis and prognosis of pancreatic cancer. *Clin Chem* 2012;58:610–8.
11 Lu TX, Sherrill JD, Wen T, *et al*. MicroRNA signature in patients with eosinophilic esophagitis, reversibility with glucocorticoids, and assessment as disease biomarkers. *J Allergy Clin Immunol* 2012;129:1064–593.
12 Gregory PA, Bracken CP, Bert AG, *et al*. MicroRNAs as regulators of epithelial-mesenchymal transition. *Cell Cycle* 2008;7:3112–7.
13 Rajasekaran S, Rajaguru P, Sudhakar Gandhi PS. MicroRNAs as potential targets for progressive pulmonary fibrosis. *Front Pharmacol* 2015;6:254.
14 Fabre A, Borie R, Debray MP, *et al*. Distinguishing the histological and radiological features of cystic lung disease in Birt-Hogg-Dubé syndrome from those of tobacco-related spontaneous pneumothorax. *Histopathology* 2014;64:741–9.
15 Goncharova EA, Goncharov DA, James ML, *et al*. Folliculin controls lung alveolar enlargement and epithelial cell survival through E-cadherin, LKB1, and AMPK. *Cell Rep* 2014;7:412–23.
16 MacDuff A, Arnold A, Harvey J, *et al*. Management of spontaneous pneumothorax: British thoracic Society pleural disease guideline 2010. *Thorax* 2010;65(Suppl 2):ii18–31.
17 Paraskevopoulou MD, Georgakilas G, Kostoulas N, *et al*. DIANA-microT web server v5.0: service integration into miRNA functional analysis workflows. *Nucleic Acids Res* 2013;41:W169–73. (Web Server issue).
18 Reczko M, Maragkakis M, Alexiou P, *et al*. Functional microRNA targets in protein coding sequences. *Bioinformatics* 2012;28:771–6.
19 Furuya M, Tanaka R, Koga S, *et al*. Pulmonary cysts of Birt-Hogg-Dubé syndrome: a clinicopathologic and immunohistochemical study of 9 families. *Am J Surg Pathol* 2012;36:589–600.
20 Jinnin M, Ihn H, Tamaki K. Characterization of SIS3, a novel specific inhibitor of Smad3, and its effect on transforming growth factor-beta1-induced extracellular matrix expression. *Mol Pharmacol* 2006;69:597–607.
21 Wang H, Graves MW, Zhou H, *et al*. 2-Amino-4-(3,4-(methylenedioxy)benzylamino)-6-(3-methoxyphenyl)pyrimidine is an anti-inflammatory TLR-2, -4 and -5 response mediator in human monocytes. *Inflamm Res* 2016;65:61–9.
22 Hinz B. The role of myofibroblasts in wound healing. *Curr Res Transl Med* 2016;64:171–7.
23 Stone RC, Pastar I, Ojeh N, *et al*. Epithelial-Mesenchymal transition in tissue repair and fibrosis. *Cell Tissue Res* 2016;365:495–506.
24 Agarwal PP, Gross BH, Holloway BJ, *et al*. Thoracic CT findings in Birt-Hogg-Dube syndrome. *AJR Am J Roentgenol* 2011;196:349–52.
25 Park HJ, Park CH, Lee SEYang S, Park C, *et al*. Birt-Hogg-Dube syndrome prospectively detected by review of chest computed tomography scans. *PLoS One* 2017;12:e0170713.
26 Scott RM, Henske EP, Raby B, *et al*. Familial pneumothorax: towards precision medicine. *Thorax* 2018;73:270–6.
27 Park HJ, Park CH, Lee SE, *et al*. Birt-Hogg-Dube syndrome prospectively detected by review of chest computed tomography scans. *PLoS One* 2017;12:e0170713.
28 Johannesma PC, Reinhard R, Kon Y, *et al*. Prevalence of Birt-Hogg-Dubé syndrome in patients with apparently primary spontaneous pneumothorax. *Eur Respir J* 2015;45:1191–4.
29 Graham RB, Nolasco M, Peterlin B, *et al*. Nonsense mutations in folliculin presenting as isolated familial spontaneous pneumothorax in adults. *Am J Respir Crit Care Med* 2005;172:39–44.
30 Ishii H, Oka H, Amemiya Y, *et al*. A Japanese family with multiple lung cysts and recurrent pneumothorax: a possibility of Birt-Hogg-Dubé syndrome. *Intern Med* 2009;48:1413–7.
31 Xing H, Liu Y, Jiang G, *et al*. Clinical and genetic study of a large Chinese family presented with familial spontaneous pneumothorax. *J Thorac Dis* 2017;9:1967–72.

32 Iwabuchi C, Ebana H, Ishiko A, *et al*. Skin lesions of Birt-Hogg-Dubé syndrome: clinical and histopathological findings in 31 Japanese patients who presented with pneumothorax and/or multiple lung cysts. *J Dermatol Sci* 2018;89:77–84.
33 Sattler EC, Lang MU, van Steensel MAM, *et al*. Late onset of skin manifestations in Birt-Hogg-Dubé syndrome with FLCN mutation p.W260X. *Acta Derm Venereol* 2012;92:187–8.
34 Steinlein OK, Ertl-Wagner B, Ruzicka T, *et al*. Birt-Hogg-Dubé syndrome: an underdiagnosed genetic tumor syndrome. *J Dtsch Dermatol Ges* 2018;16:278–83.
35 Pavlovich CP, Grubb RL, Hurley K, *et al*. Evaluation and management of renal tumors in the Birt-Hogg-Dubé syndrome. *J Urol* 2005;173:1482–6.
36 Chiu HT, Garcia CK. Familial spontaneous pneumothorax. *Curr Opin Pulm Med* 2006;12:268–72.
37 Starling GP, Yip YY, Sanger A, *et al*. Folliculin directs the formation of a Rab34-RILP complex to control the nutrient-dependent dynamic distribution of lysosomes. *EMBO Rep* 2016;17:823–41.
38 Dodding MP. Folliculin - A tumor suppressor at the intersection of metabolic signaling and membrane traffic. *Small GTPases* 2017;8:100–5.
39 Latifkar A, Ling L, Hingorani A, *et al*. Loss of sirtuin 1 alters the secretome of breast cancer cells by impairing lysosomal integrity. *Dev Cell* 2019;49:393–408.